PROPERTIES OF MANGANESE ORES AND THEIR CHANGE IN THE PROCESS OF CALCINATION

B. Sorensen[1], S. Gaal[2], M. Tangstad[1], E. Ringdalen[2], R. Kononov[3] and O. Ostrovski[3]

[1] NTNU, 7491 Trondheim, Norway, bjorn.sorensen@ntnu.no; Merete.Tangstad@material.ntnu.no
[2] SINTEF, Materials and Chemistry, 7465 Trondheim, Norway, sean.gaal@sintef.no,
eli.ringdalen@sintef.no
[3] School of Materials Science and Engineering, the University of New South Wales, UNSW Sydney,
NSW 2052, Australia, o.ostrovski@unsw.edu.au

ABSTRACT

The paper presents results of a study of the properties of Wessels, Groote Eylandt, CVRD, and Gabonese manganese ores and their change in the process of calcinations in different gas atmospheres.

Wessels and Groote Eylandt manganese ores were examined at the University of New South Wales (Australia) using XRD, optical, SEM and EPMA analyses; CVRD and Gabonese ores were studied at SINTEF and NTNU (Norway) using quantitative XRD analysis. The manganese ores had significant differences in chemistry and mineralogy. Equilibrium phases in ores at temperatures of 800°C, 1000°C and 1200°C in different gas atmospheres were examined using FACTSage software. The calculated phase composition was in agreement with quantitative XRD analysis.

In the process of calcination of manganese ores in air, MnO_2 was reduced to Mn_2O_3 and Mn_3O_4, while during calcination in a reducing atmosphere manganese oxides were reduced to MnO and iron oxides to metallic iron. Formation of a liquid slag in ores at equilibrium was predicted for Wessels, Groote Eylandt and Gabonese ores at 1200°C in air and 1000-1200°C in a reducing atmosphere. No liquid slag was predicted for equilibrium phases in CVRD ore.

1 INTRODUCTION

Industrial manganese ores vary significantly in chemistry and mineralogy. It is well-known that the properties of a manganese ore have a large influence on the technology and efficiency of the production of manganese alloys.

The melting and reduction behaviour of ores are defined by their chemistry, mineralogy and physical properties, which change as the ore is heated in a reducing atmosphere in a ferroalloy furnace.

Mineralogy and geology of manganese ores have been presented in a number of publications which are reviewed by Varentsov and Grasselly [1]. Wessels and Groote Eylandt ores were studied by Gutzmer and Beukes [2] and Ostwald [3] correspondingly, among others. However, the change in the ore chemistry and mineralogy upon heating has only been examined to a limited extent. Kang et al. [4] studied equilibrium phases in the $CaO\text{-}MnO\text{-}Al_2O_3\text{-}SiO_2$ system. They also analysed experimental data presented in literature. A number of phases were identified in this system [4]: slag (molten oxide phase), olivine, tephroite, monoxide, rhodonite, galaxite, anorthite and others, depending on the temperature and chemistry. Zhao et al. [5] examined equilibrium phases in the $CaO\text{-}MnO\text{-}Al_2O_3\text{-}SiO_2\text{-}K_2O$ system. They demonstrated that K_2O strongly affected the melting properties of the oxide system. Experimentally, these systems were analysed by equilibrating with a metal phase (Mn [4] or Mn-Si alloy [5]) at a given temperature in an inert atmosphere and quenching. These conditions were strongly reducing which can be referred to the smelting/reduction conditions in the ferroalloy furnace.

The focus of this paper is on the phase composition of the ore in the temperature range 800-1200°C when the ore is exposed to the CO gas; under these conditions manganese oxides are reduced only to MnO. The paper also studies the phases formed in this temperature range in air, as these conditions are relevant to the sintering process

This paper analyses chemical and phase composition of CVRD, Gabonese, Wessels and Groote Eylandt ores and their change upon heating in different gas atmospheres. Equilibrium phases formed upon heating in air and in a reducing atmosphere were analysed using FACTSage software. The aim of this study is to establish the behaviour of the ore upon heating and define a temperature range in which the ore is solid.

2 EXPERIMENTAL

Wessels and Groote Eylandt ores were examined at the University of New South Wales (UNSW), Australia; CVRD and Gabonese ores were studied at SINTEF and the Norwegian University of Science and Technology (NTNU), Norway.

The ores were ground into different particle size fractions. The size fraction of Wessels and Groote Eylandt manganese ores was 45 -150 μm; CVRD and Gabonese ores were studied in the range 100 – 300 μm. Chemical composition of the ores was determined by XRF, as given in Table 1 (moisture and LOI were excluded).

Table 1: Chemical composition of manganese ores

Ore	Chemical composition, wt%							
	MnO	FeO	SiO_2	Al_2O_3	CaO	MgO	BaO	K_2O
Wessels	70.0	14.4	4.18	1.51	8.34	0.73	0.82	-
Groote Eylandt	81.9	5.80	6.09	3.90	0.18	<0.1	0.49	1.53
CVRD	66.0	12.9	9.01	10.3	0.21	0.36	0.24	0.97
Gabonese	83.1	2.68	5.85	7.1	0.08	<0.01	0.22	0.93

Samples of manganese ore at UNSW were subjected to XRD, optical and electron microscope analyses. XRD analysis was done using a Siemens D5000 X-Ray diffractometer. The XRD patterns were analysed qualitatively using “Traces” software from Diffraction Technology Pty. Ltd., with JCPDS-PDF2 database**.**

In the XRD analysis at NTNU (Bruker D8 advance with a wavelength dispersive detector SolX), variable slits (V20) were used to achieve better signal peaks at higher angles and to reduce the collection time. Rietveld refinement with TOPAS 4 software was used for quantitative XRD analysis. Literature data on the nsutite structure were insufficient for the rietveld analysis; this phase was assessed by direct area fraction measurements using peak positions from the space group and lattice parameters combined with information on relative peak intensities from published Nsutite diffractograms (pattern 00-017-0510 in the JCPDS-PDF2 powder diffraction database).

Samples for optical and electron microscope analyses were prepared by mounting in an epoxy resin mould. The samples were held within a vacuum chamber for around 30 minutes before being left to harden for around 24 hours.

The samples were then ground using SiC paper, from 120 to 4000 grade; followed by 4 μm, 1 μm and 0.5 μm diamond paste on a polishing wheel. The samples were washed using soap and water in an ultrasonic bath between the grinding and polishing, before being rinsed under ethanol.

Optical photomicrographs were obtained using a Nikon Epiphot 200 (Nikon Corp., Japan) inverted stage metallurgical microscope with an attached Nikon DXM1200 digital camera. Images were captured using the Nikon ACT-1 software package.

Samples were coated with carbon for SEM, EDS and EPMA analysis. SEM was carried out using a high resolution (1.5 nm) Hitachi S-4500 field emission SEM (FESEM) with a tilting stage, Robinson back-scatter detector and Oxford Instruments cathodoluminescence detector (MonoCL2/ ISIS).

Energy dispersive X-ray spectroscopy (EDS) was done using an Oxford Instruments Isis energy dispersive x-ray analyser. This was used to perform qualitative and semi-quantitative chemical analysis at different points and areas within the samples.

The mounted samples were analysed using a Cameca SX-50 electron microprobe. Standard operating procedure involved a 15 kV accelerating voltage, 1-3μm beam size and a 20nA beam current. The microprobe has four multi-crystal wavelength-dispersive spectrometers and was operated with a configuration involving two TAP, one LIF and one PET diffracting crystals.

Equilibrium phases in Gabonese, CVRD, Wessels and Groote Eylandt ores in the temperature range 800-1200°C in air and reducing gas atmosphere (CO for Gabonese and CVRD ores and H_2 for Wessels and Groote Eylandt ores) were calculated using FACTSage software (version 6.0 with a database developed by Tang and Olsen [6]).

3 RESULTS

3.1 Wessels Ore

Wessels ore contained a relatively high amount of iron and calcium, low silicon and alkalis (Table 1). XRD analysis identified the following phases in the Wessels ore: bixbyite, braunite, manganite, hausmannite and calcite. Braunite was found in two modifications - with high silica and low silica [3]. The Mn/Fe weight ratio in the ore was 4.85. In the high silica braunite (8-10 at% Si), the Mn content was relatively small, 14-20 at%; this phase is also characterised by high iron (4.5-6.5 at%) and calcium (8-10 at%) content. Iron was also detected in the other phases, except calcite.

The XRD analysis of sintered samples showed that in hydrogen, the manganese oxides in the ore were reduced to MnO and iron oxides to metallic iron (Figure 1). This corresponds to 45% of the ore reduction (the degree of reduction defined as percentage of oxygen removed from manganese and iron oxides, was estimated from the sample's weight change in the reduction process).

XRD patterns of samples sintered in air and argon were almost the same and showed that Mn_2O_3 and MnO(OH) were converted to Mn_3O_4.

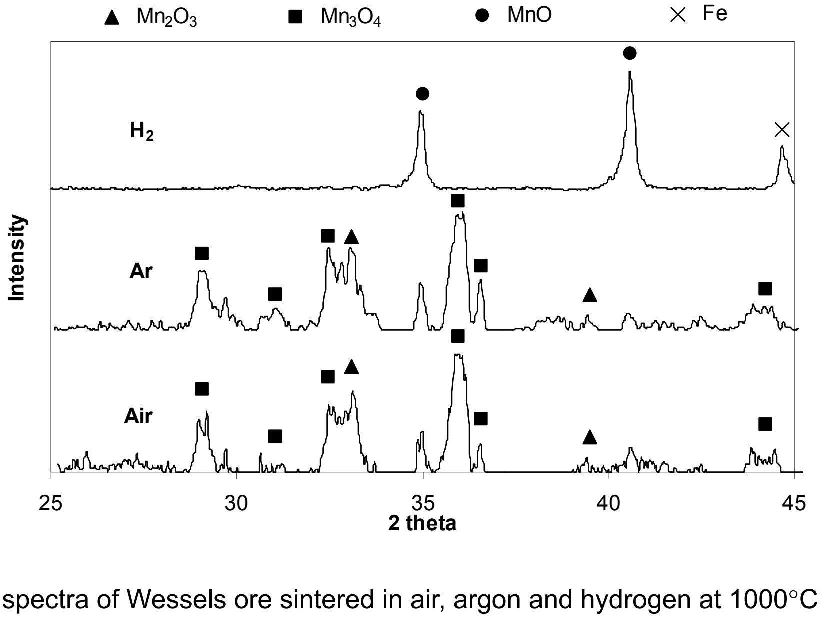

Figure 1: XRD spectra of Wessels ore sintered in air, argon and hydrogen at 1000°C for 30 min

Equilibrium phases in Wessels ore heated to 800-1200°C in air and hydrogen are presented in Table 2. Major phases in Wessels ore heated to 1000°C in air in accordance with XRD analysis were Mn_2O_3 and Mn_3O_4; Wessels ore calcined at this temperature in hydrogen consisted of MnO and metallic iron. The same major phases were predicted by the FACTSage analysis. Minor phases, expected from the FACTSage analysis in the ore sintered in air, merwinite and Ca_2SiO_4 were slightly above 5 wt%; $Ca_2Fe_2O_5$ was below 4 wt%; their identification at UNSW was not reliable. However, the calculated amount of the Ca_2SiO_4 phase in the ore reduced in hydrogen exceeded 10 wt%, although it was not detected by XRD.

No liquid slag was predicted in Wessels ore heated in reducing gas to 1200°C, although it is expected when heated to this temperature in air. The liquid slag contained 45.5 wt% Fe_2O_3 and 21.6 wt% Mn_2O_3.

Table 2: Equilibrium phases in Wessels ore heated in air and H_2 to 800-1200°C

Atmosphere	Temperature, °C	Phases
Air	800	**Bixbyite, 84.0% Mn_2O_3**, merwinite $MgO.3CaO.Si_2O_4$, Ca_2SiO_4, $Ca_2Fe_2O_5$, $BaO.Al_2O_3$ ($2BaO.SiO_2$)
	1200	**Tetragonal spinel, 61.6% Mn_3O_4,** Liquid slag (45.5% Fe_2O_3, 21.6% Mn_2O_3), Ca_2SiO_4, merwinite $MgO.3CaO.Si_2O_4$, $BaO.Al_2O_3$ (Al-spinel, 88.7% $MnAl_2O_4$)
H_2	800	**Monoxide (Mn,Fe,Ca,Mg)O, 96.4% MnO**, Ca_2SiO_4, Fe, Al-spinel, 99.8% $MnAl_2O_4$ ($2BaO.SiO_2$).
	1200	**Monoxide (Mn,Fe,Ca,Mg)O, 95.7% MnO**, Ca_2SiO_4, Fe, Al-spinel, 99.8% $MnAl_2O_4$, ($2BaO.SiO_2$).

Note. In bold: major phases; in brackets: minor phases, less than 1 wt%; phases are presented in the descending (mass) order.

3.2 Groote Eylandt Ore

Groote Eylandt (GE) ore is a high-grade ore with a manganese content of 55 wt% (71 wt% MnO). The only phase identified in GE ore by XRD was MnO_2 (pyrolusite). However, optical analysis and SEM revealed the complex mineralogical structure of the ore. Apart from pyrolusite, GE ore contained iron silicate and silica; pyrolusite grains were distinguished by the colour given by different impurities.

Manganese was mainly present as pyrolusite and cryptomelane. Iron was found in the form of iron alumo-silicates and in small amounts in the manganese oxides. Silicon was present in the form of quartz inclusions, in iron alumo-silicate, and also in manganese oxide. Potassium was observed in the form of cryptomelane, it was also detected in iron alumo-silicate.

Behaviour of GE ore upon heating was studied in air, argon and hydrogen at a temperature of 1000°C. The phase development during sintering in air and hydrogen examined by XRD analysis, is shown in Figures 2 and 3 correspondingly. FACTSage equilibrium phases in GE ore heated to 800-1200°C in air and hydrogen are presented in Table 3.

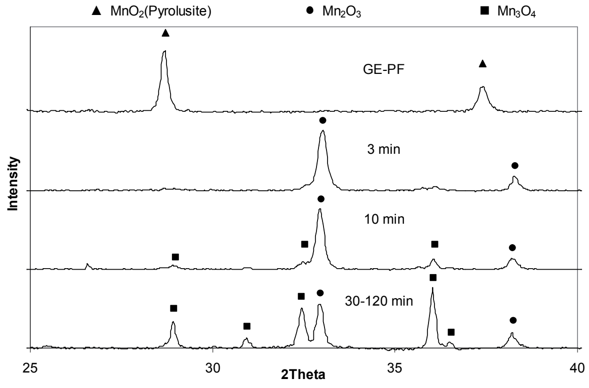

Figure 2: XRD spectra of Groote Eylandt ore sintered at 1000°C in air

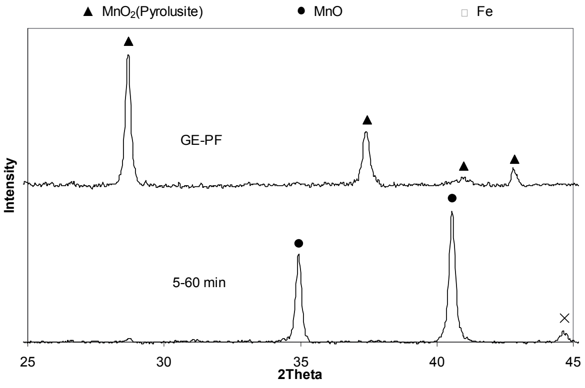

Figure 3: XRD spectra of Groote Eylandt ore sintered at 1000°C in hydrogen

Pyrolusite MnO_2 in GE ore, upon heating and holding at 1000°C, was reduced to Mn_2O_3 and Mn_3O_4 in both air and argon. MnO_2 became invisible in the XRD spectra after 3 min of sintering. The Mn_3O_4 fraction increased and Mn_2O_3 decreased with increasing sintering time. Only Mn_3O_4 was detected in the sample sintered in argon for 70 min.

The same major phases in air at 1000°C, Mn_3O_4 and Mn_2O_3, were calculated by FACTSage. Minor phases included leucite and garnet (below the detectable level).

When GE ore was sintered in hydrogen at 1000°C, higher manganese oxides were reduced to MnO, and iron oxides were reduced to metallic iron. Formation of liquid slag (manganese alumino-silicate melt with 3.5 wt% K_2O) was predicted by FACTSage calculations but was not observed in the spectra. This phase could be amorphous. Another possible reason, common to all systems, was that the holding time was not sufficient to reach the equilibrium state.

Table 3: Equilibrium phases in Groote-Eylandt ore heated in air and H_2 to 800-1200°C

Atmosphere	Temperature, °C	Phases
Air	800	**Bixbyite, 92.0% Mn_2O_3**, leucite $KAlSi_2O_6$, garnet $Mn_3Al_2Si_3O_{18}$; ($BaO.SiO_2$, wollastonite $(Ca,Mn)SiO_3$, 12.3% $MnSiO_3$)
	1200	**Tetragonal spinel Mn_3O_4,** Liquid slag (49.4% MnO), leucite $KAlSi_2O_6$, (galaxite $MnAl_2O_4$, anorthite $CaAl_2Si_2O_8$, $BaO.SiO_2$)
H_2	800	**Monoxide (Mn,Fe,Ca)O, 99.4% MnO**, Mn_2SiO_4, kaliophilite $KAlSiO_4$, Fe, galaxite $MnAl_2O_4$, ($BaO.SiO_2$).
	1200	**Monoxide (Mn,Fe,Ca)O, 99.3% MnO**, **Liquid slag** (61.4% MnO, 22.6% SiO_2, 13.6% Al_2O_3, 1.64% K_2O), Fe, $KAlSiO_4$ – kaliophilite, Mn_2SiO_4 (galaxite $MnAl_2O_4$, $BaO.SiO_2$).

3.3 CVRD ore

CVRD ore phases and their relative concentrations found by the Rietveld analysis are listed in Table 4. The main manganese containing phase was nsutite. Nsutite has poor crystallinity;published crystal structure for nsutite is incomplete. Quantification of peak intensities requires accurate atomic positions, which are unknown. The quantity of nsuitite was estimated by area fraction measurement using peak positions from the space group and lattice parameters combined with information on relative peak intensities from published Nsutite diffractograms (pattern 00-017-0510 in the JCPDS-PDF2 powder diffraction database). CVRD ore contained a relatively high concentration of alumina which was observed in three phases: gibbsite, kaolinite and lithiophorite.

Quantitative phase analyses of CVRD ore heated in air and CO at 800°C (8 hours holding time) and 1200°C (4 hours holding time) are presented in Table 5.

The phases in samples of CVRD ore processed in air at 800°C and 1200°C were visibly different. The dominant phase in the sample heated to 1200°C was tetragonal spinel ($\mathbf{Mn^{2+}}$)(Fe^{3+}, Al^{3+}, $\mathbf{Mn^{3+}}$)$_2O_4$ in which hausmannite was a major component. In the sample heated to 800°C, manganese predominantly existed in the Mn^{3+} state in the composition of bixbyite and jacobsite.

The phase compositions of samples of CVRD ore heated in CO to 800°C and 1200°C were about the same. There were however small differences The sample processed at 800oC contained graphite formed as a result of solid carbon deposition from CO; galaxite in this sample had poor crystalinity. The sample heated to 1200°C did not contain graphite and had galaxite with higher crystalinity.

Equilibrium phases in CVRD ore calculated using FACTSage at 800-1200°C in air and CO are presented in Table 6.

Table 4: Quantitative rietveld analysis of the CVRD raw ore

Mineral	Formula	Wt %
Pyrolusite	MnO_2	3.0
Gibbsite	$Al(OH)_3$	1.4
Quartz	SiO_2	1.8
Cryptomelane	$K_xMn^{4+}_{8-x}Mn^{2+}_xO_{16}$	13.7
Kaolinite(BISH)	$Al_2Si_2O_5(OH)_4$	15.2
Hematite	Fe_2O_3	5.8
Todorokite	$(Mn^{2+},Ca,Na,K)(Mn^{4+},Mn^{2+},Mg)_6O_{12} \bullet 3H_2O$	18.3
Lithiophorite	$(Al,Li)Mn^{4+}O_2(OH)_2$	5.3
Nsutite	$Mn^{4+}_{1-x}Mn^{2+}_xO_{2-2x}OH_{2x}$, where x = 0.06-0.07	35.5

Table 5: Quantitative rietveld analysis of CVRD ore heated in air and CO at 800°C (8 hours) and 1200°C (4 hours)

Conditions	Mineral	Formula	Wt%
800°C, Air	Bixbyite	$(\mathbf{Mn}, Fe)_2O_3$	36.6
	Jacobsite	$(\mathbf{Mn^{2+}}, \mathbf{Fe^{2+}}, Mg^{2+})(\mathbf{Fe^{3+}}, \mathbf{Mn^{3+}}, Al^{3+})_2O_4$	34.5
	Hausmannite	$(Mn^{2+})(Mn^{3+})_2O_4$	24.0
	Braunite -1	$(Mn^{2+})(Mn^{3+})_6SiO_{12}$	4.1
	Quartz	SiO_2	<1
1200°C, Air	Tetragonal spinel	$(Mn^{2+})(\mathbf{Mn^{3+}}, Al^{3+}, Fe^{3+})_2O_4$	87.8
	Jacobsite	$(Mn^{2+})(\mathbf{Fe^{3+}}, \mathbf{Mn^{3+}}, Al^{3+})_2O_4$	10.2
	Kalsilite	$KAlSiO_4$	1.4
	Spinel	$MgAl_2O_4$	<1
800°C, CO	Manganosite	$(\mathbf{Mn}, Fe)O$	47.2
	Tephroite	$(\mathbf{Mn}, Mg, Fe)_2SiO_4$	29.0
	Galaxite	$(\mathbf{Mn^{2+}}, Fe^{2+}, Mg^{2+})(\mathbf{Al}, Fe^{3+})_2O_4$	20.6
	"Iron alpha"	Fe	2.0
	Quartz	SiO_2	<1
	Graphite-3R	C	<1
	Unidentified	?	1.6
1200°C, CO	Tephroite	$(\mathbf{Mn}, Mg, Fe)_2SiO_4$	36.4
	Manganosite	$(\mathbf{Mn}, Fe)O$	34.8
	Galaxite	$(\mathbf{Mn}, Mg, Fe)Al_2O_4$	18.9
	Olivine	$(Mg, Fe)_2SiO_4$	6.4
	Iron alpha	Fe	3.3
	Brucite	$Mg(OH)_2$	<1

Table 6: Equilibrium phases in CVRD ore heated in air and CO to 800-1200°C

Atmosphere	Temperature, °C	Phases
Air	800	**Bixbyite, 85.3% Mn_2O_3**, leucite $KAlSi_2O_6$, garnet $Mn_3Al_2Si_3O_{12}$ (anorthite $CaAl_2SiO_8$, olivine $(Mn,Mg)_2SiO_4$)
	1200	**Tetragonal spinel (Mn_3O_4)**, leucite $KAlSi_2O_6$, $MnAl_2O4$ – galaxite, garnet $Mn_3Al_2Si_3O_{12}$, Al-spinel, 70.5% $MnAl_2O_4$ (anorthite $CaAl_2SiO_8$, olivine $(Mn,Mg)_2SiO_4$)
CO	800	**Monoxide (Mn,Fe,Mg)O, 89.9% MnO**, olivine $(Mn,Mg)_2SiO_4$, 78.1% Mn_2SiO_4, galaxite $MnAl_2O_4$, kaliophilite $KAlSiO_4$, graphite.
	1200	**Monoxide (Mn,Fe,Mg)O, 94.0% MnO**, olivine $(Mn,Mg)_2SiO_4$, 86.3% Mn_2SiO_4, galaxite $MnAl_2O_4$, kaliophilite $KAlSiO_4$, Fe.

Major phases in the ore heated in air, bixbyite at 800°C and tetragonal spinel at 1200°C, were observed in the XRD spectra and also predicted by FACTSage analysis, although there is a discrepancy in the overall phase composition of the CVRD ore. Probably the holding time of 8 hours at 800°C and 4 hours at 1200°C was not sufficient to reach phase equilibrium in air. XRD and FACTSage phase analyses gave very close phase compositions for the ore heated in CO. Calculations showed that a monoxide, which was 90-95 wt% MnO, was a major phase at all three temperatures with olivine (78-86 wt% Mn_2SiO_4) being the second largest phase. The same phases were observed in the XRD spectra at 1200°C; monoxide phase and tephroite were present in about the same amount. No liquid phase was observed or predicted in CVRD ore in the temperature range 800-1200°C.

3.4 Gabonese ore

Quantitative XRD analysis of Gabonese ore is given in Table 7. Major Mn-containing phases were cryptomelane, nsutite and pyrolusite. Alumina was found in lithiophorite; only traces of gibbsite were observed. Iron oxide in this ore was present in the form of hematite and goethite, although in small amounts.

Table 7: Quantitative rietveld analysis of Gabonese ore

Mineral	Formula	Wt %
Cryptomelane	$K_x(Mn^{4+})_{8-x}(Mn^{3+})_xO_{16}$	35.32
Nsutite	$(Mn^{4+})_{1-x}(Mn^{2+})_xO_{2-2x}OH_{2x}$, where x = 0.06-0.07	32.57
Pyrolusite	MnO_2	12.42
Lithiophorite	$(Al,Li)Mn^{4+}O_2(OH)_2$	7.40
Quartz	SiO_2	5.92
Goethite	FeO(OH)	3.01
Ramsdellite	MnO_2	1.87
Hematite	Fe_2O_3	1.47
Gibbsite	$Al(OH)_3$	<1

Quantitative phase analyses of Gabonese ore heated in air and CO at 800°C (8 hours holding time) and 1200°C (4 hours holding time) are presented in Table 8.

Changes in the phase composition upon heating of Gabonese ore in air and CO followed trends observed for CVRD ore. In air, pyrolusite was converted to bixbyite and hausmannite at 800°C; hausmannite (tetragonal spinel) became the prevailing phase at 1200°C. When the ore was heated in a CO atmosphere, higher manganese oxides were reduced to manganosite. Quartz which was observed in the XRD spectra at 800°C, disappearing at 1200°C and forming tephroite.

Table 8: Quantitative rietveld analysis of Gabonese ore heated in air and CO at 800°C (8 hours) and 1200°C (4 hours)

Conditions	Mineral	Formula	Wt%
800^{o}C, Air	Hausmannite	$(Mn^{2+})(Mn^{3+})_2O_4$	59.4
	(Maghemite)	gamma -$(Mn, Fe)_2O_3$	16.0
	Bixbyite	$(\mathbf{Mn}, Fe)_2O_3$	11.7
	Quartz	SiO_2	7.0
	Jacobsite	$(\mathbf{Mn^{2+}}, Fe^{2+})(\mathbf{Fe^{3+}}, \mathbf{Mn^{3+}}, Al^{3+})O_4$	3.5
	Iwakiite	$(Mn^{2+}, Fe^{2+})(Fe^{3+}, Mn^{3+}, Al^{3+})O_4$	2.3
1200°C, Air	Tetragonal spinel	$(Mn^{2+})(\mathbf{Mn^{3+}}, Al^{3+}, Fe^{3+})_2O_4$	84.6
	Jacobsite	$(Mn^{2+}, Fe^{2+})(Fe^{3+}, Mn^{3+}, Al^{3+})_2O_4$	3.6
	Leucite	$KAlSi_2O_6$	3.1
	Galaxite	$(\mathbf{Mn}, Mg, Fe)(\mathbf{Al}, Fe^{3+})_2O_4$	1.4
	Unidentified	?	7.2
800°C, CO	Manganosite	$(\mathbf{Mn},Fe)O$	76.2
	Galaxite	$(\mathbf{Mn}, Mg, Fe)(\mathbf{Al}, Fe^{3+})_2O_4$	14.4
	Quartz	SiO_2	8.7
	Iron alpha	Fe	<1
	Graphite-3R	C	<1
1200°C, CO	Manganosite	$(\mathbf{Mn}, Fe)O$	56.3
	Tephroite	$(\mathbf{Mn}, Mg, Fe)_2SiO_4$	24.3
	Spinel	$(\mathbf{Mn}, Mg, Fe)(\mathbf{Al}, Fe^{3+})_2O_4$	8.6
	Iron alpha	Fe	1.4
	Unidentified	?	9.4

Calculated equilibrium phases in Gabonese ore presented in Table 9 are generally in agreement with the XRD analysis. The unidentified phase in the XRD spectra of Gabonese ore heated to 1200°C in both air and CO may originate from molten slag, which was predicted by the FACTSage calculations.

Table 9: Equilibrium phases in Gabonese ore heated in air and CO to 800-1200°C

Atmosphere	Temperature, °C	Phases
Air	800	**Bixbyite, 90.8%** $\mathbf{Mn_2O_3}$, leucite $KAlSi_2O_6$, garnet $Mn_3Al_2Si_3O_{12}$ (anorthite $CaAl_2SiO_8$, $BaO.SiO_2$)
	1200	**Tetragonal spinel, 77.5%** $\mathbf{Mn_3O_4}$, galaxite $MnAl_2O_4$, Liquid slag (50.4% MnO), leucite $KAlSi_2O_6$, garnet $Mn_3Al_2Si_3O_{12}$ ($BaO.SiO_2$)
CO	800	**Monoxide (Mn,Fe,Ca)O, 94.7% MnO**, olivine $(Mn,Mg)_2SiO_4$, 89.3% Mn_2SiO_4, galaxite $MnAl_2O_4$, kaliophilite $KAlSiO_4$, graphite, ($BaO.SiO_2$).
	1200	**Monoxide (Mn,Fe,Mg)O, 96.5% MnO**, Liquid slag (57.3% MnO), galaxite $MnAl_2O_4$, Fe, ($2BaO.SiO_2$).

4 DISCUSSION

Manganese ores of different origin have a different chemistry and mineralogy, which affect their melting and reduction properties. Literature covers the mineralogy of original ores[1-3] and composition and melting properties of slags [4,5], while changes in the phase composition of manganese ores upon heating have not been reported. The slag liquidus temperature, $T_{L,}$ changes in a complex manner with changing chemistry. For example, an increase in the silica concentration to 10 wt% increases T_L for CaO/Al_2O_3 ratio 0.5-1 and decreases T_L when the CaO/Al_2O_3 ratio is 2 [4] the effect of K_2O on the liquidus temperature depends on manganese oxide content and CaO/Al_2O_3 ratio

[5]. Understanding the melting properties of ore requires data on the phase composition and its change during the process of heating, which depends on the gas atmosphere.

Analysis of changes in the phase composition of Wessels and Groote Eylandt ores at UNSW was qualitative; it established that MnO_2 was reduced to Mn_2O_3 and Mn_3O_4 when the ore was heated in air and to MnO when it was heated in a hydrogen atmosphere. Iron oxides were reduced by hydrogen to metallic iron. The same changes were observed in the phase composition of CVRD and Gabonese ores at NTNU/SINTEF. Quantitative XRD analysis was not accurate as some phases had poor crystallinity; nevertheless it gave more detailed information on phase change in the process of heating of ores, particularly in a reducing CO atmosphere.

In general results of equilibrium calculations using FACTSage in a reducing atmosphere and XRD analysis were in a good agreement. This indicates that the ore samples studied in a reducing atmosphere were close to equilibrium. A good correlation was also observed between the experimentally determined and calculated major phases in the ore heated in air, although a discrepancy was observed for minor phases. This can be explained by poor crystallinity of some phases and insufficient holding time in air to reach equilibrium, as can also be expected during the industrial processing of manganese ores.

In the original ore, manganese naturally existed in the oxidising Mn^{4+} state, in the form of pyrolusite, nsutite, bixbyite or braunite. In Groote Eylandt, CVRD and Gabonese ores which contain K_2O (0.9-1 wt% K_2O in CVRD and Gabonese ores and 1.5 wt% K_2O in GE ore), a significant fraction of Mn^{4+} was found in the form of cryptomelane. Upon heating, Mn^{4+} was reduced to Mn^{3+} and Mn^{2+}, with a significant effect on the ore phase composition. Potassium oxide reacted with silica and alumina forming leucite $KAlSi_2O_6$ and/ore kaliophilite $KAlSiO_4$; these compounds have a high melting temperature (1693°C for leucite [7]). When the ore was heated in a reducing atmosphere, higher manganese oxides were reduced to MnO which with silica and other oxides formed tephroite with a relatively low melting temperature. Potassium oxide, partially dissolved in this silicate phase, decreased its melting temperature, forming liquid slag.

Both CVRD and Gabonese ores contained a high concentration of alumina. In a reducing atmosphere, alumina with MnO formed galaxite, detected by XRD analysis and predicted by the calculation of equilibrium phases using FACTSage.

No liquid phase was observed or predicted in CVRD ore heated up to 1200°C in air or reducing atmosphere. XRD analysis of sintered CVRD ore detected tephroite phase and an unidentified phase; both of them were molten at the sintering temperature (≈1450°C). Formation of liquid slag in ores at equilibrium was predicted for Gabonese and GE ores in air at 1200°C. Under reducing conditions, molten slag was predicted in Groote Eylandt and Gabonese ores at 1000-1200°C, although a major phase was solid monoxide (predominately, MnO). A liquid phase, even a small amount, can affect material flow in the furnace. No MnO reduction to metal phase is expected at these temperatures.

5 CONCLUSIONS

Analysis of Wessels, Groote Eylandt, CVRD and Gabonese manganese ores revealed their diverse chemical composition and complex mineralogical structure.

The following phases in the original ore were identified by XRD and EPMA analyses at UNSW and quantitative XRD analysis at NTNU/SINTEF.

- Wessels ore: bixbyite, braunite, manganite, hausmannite and calcite;
- GE ore: pyrolusite, cryptomelane manganese and iron silicates, and silica;
- CVRD ore: nsutite, todorokite, cryptomelane, gibbsite, quartz, kaolinite, hematite and lithiophorite;
- Gabonese ore: nsutite, cryptomelane, gibbsite, quartz, ramsdellite, hematite, goethite and lithiophorite.

Upon sintering in air, MnO_2 was reduced to Mn_2O_3 and Mn_3O_4, sintering of manganese ores in hydrogen reduced higher manganese oxides to MnO and iron oxides to metallic iron.

Calculated equilibrium phases using FACTsage for ores heated under a reducing gas atmosphere were in agreement with XRD analysis. Formation of liquid slag in ores at equilibrium was predicted for Wessels ore at 1200°C in air; Groote Eylandt ore at 1200°C in air and 1000-1200°C in a reducing atmosphere; Gabonese ore at 1200°C in air and 1000-1200°C in a reducing atmosphere; no liquid slag was observed in equilibrium phases in CVRD ore.

6 ACKNOWLEDGEMENTS

Authors are grateful to Dr Kai Tang for the ferromanganese alloy database and Dr S. Decterov for valuable comments. Oleg Ostrovski expresses sincere gratitude to SINTEF for hospitality during his sabbatical leave.

7 REFERENCES

[1] Varentsov, I.M. and Grasselly, G. “Geology and Geochemistry of Manganese. Volume I – General problems – Mineralogy, geochemistry, methods”, E. Schweizerbart’sche Verlagsbuchhandlung, 1980, Stuttgart.

[2] Gutzmer, J.and Beukes, N.J. “Mineral Paragenesis of the Kalahari Manganese Field, South Africa”, Ore Geology. Reviews, 11 (1996), 405-428.

[3] Ostwald, J., “Mineralogy of the Groote Eylandt Manganese Oxides”, Ore Geology. Reviews, 4 (1988), 3-45.

[4] Kang, Y.-B., Jung, In-Ho, Decterov, S.A., Pelton, A.D. and Lee, H.G. “Phase Equilibria and Thermodynamic Properties of the CaO-MnO-Al2O3-SiO2 System by Critical Evaluation, Modelling and Experiment”, ISIJ International 44 (2004), 975-983.

[5] Zhao, B., Jak, E., Hayes, P.C. “Phase Equilibria in the “MnO”-CaO-SiO2-Al2O3-K2O Relevant to Manganese Smelting Slags. International Journal of Materials Research (formerly Z. Metallkd.), 99 (2008), 888-899.

[6] Tang, K., Olsen, S.E. “Computer Simulation of Equilibrium Relations in Manganese Ferroalloy Production”, Metallurgical and Materials Transactions B, 37B (2006), 599-606.

[7] Kosanovi, C., Buljan, I., Bosnar, S. et al. ”Thermal Transformation of Various Potassium Aluminosilicate Precursors”, Acta Chimica Slovenica, 55 (2008), 960–965.